

## Thermal phenomenology of hadrons from 200A GeV S+S collisions

Ekkard Schnedermann,<sup>1,2</sup> Josef Sollfrank,<sup>1</sup> and Ulrich Heinz<sup>1</sup>

<sup>1</sup>*Institut für Theoretische Physik, Universität Regensburg, D-93040 Regensburg, Germany*

<sup>2</sup>*Department of Physics, Brookhaven National Laboratory, Upton, New York 11973*

(Received 14 July 1993)

We develop a complete and consistent description for the hadron spectra from heavy ion collisions in terms of a few collective variables, in particular temperature, longitudinal, and transverse flow. To achieve a meaningful comparison with presently available data, we also include the resonance decays into our picture. To disentangle the influences of transverse flow and resonance decays in the  $m_T$  spectra, we analyze in detail the shape of the  $m_T$  spectra.

PACS number(s): 25.75.+r

### I. INTRODUCTION

Our current understanding of QCD results basically from high-energy experiments with small collision systems suffering hard interactions which are relatively easy to analyze. In a first attempt to test QCD predictions for larger systems, especially the predicted phase transition from hadronic matter to the hypothetical quark gluon plasma, existing accelerators were modified to experiment with nuclei instead of only protons. The first round of experiments with nuclear beams took place during the years 1986–1990 at the AGS (Alternating Gradient Synchrotron) of the Brookhaven National Laboratory (BNL) and at the SPS (Super Proton Synchrotron) at CERN. While the biggest possible projectile nuclei  $^{28}\text{Si}$  (BNL) and  $^{32}\text{S}$  (CERN) do not deserve the title “heavy ions,” the situation on the experimental side will considerably improve with the Au beam at BNL, which is already in operation, and the planned Pb beam for CERN which is planned for 1994. To fully utilize the new possibilities new methods for analyzing the heavy ion data have to be developed, which are capable of characterizing the physical situation over the whole range of nuclei and for both the energies at BNL and CERN.

In this paper we want to develop a phenomenological model for the hadronic matter by starting out with thermalization as the basic assumption and adding more features as they are dictated by the analysis of the measured hadronic spectra. Eventually we will show that under the assumption of collective flow almost all hadronic spectra can be described by the model. The model can be extended to a consistent hydrodynamical description [1], which provides a link to the possible initial conditions and can in turn be used to extract new information about the final state of the hadronic system [2,3].

We will start by explaining our choice of data in Sec. II. In Sec. III we define the stationary thermal model for particle emission and show its failure for the measured  $\pi^-$   $m_T$  spectra. We subsequently refine it by introducing resonances and their decay contributions to the  $m_T$  spectra of all measured hadronic species which can then be described successfully by a uniform temperature. The analysis of the rapidity distributions in Sec. IV A leads

us to the introduction of longitudinal flow. On the other hand, as shown in Sec. IV B, the existence of transverse flow cannot be established from the data. However this can be clarified by a closer theoretical investigation of the reaction prior to freeze out, which was briefly reported in [2] and will be presented in detail in [3]. Finally in Sec. V we critically assess the relevance of our model in the light of  $pp$  data and give a conclusion of our work.

### II. CHOICE OF DATA

From the large amount of data from many experimental groups at BNL and CERN, which have been measured with many different targets and projectiles from  $^{27}\text{Al}$  to  $^{184}\text{W}$  [4], we want to pick out one set of data which is, for our purpose, easiest to interpret: transverse mass and rapidity distributions of pions [5], protons [5],  $K_s^0$ ,  $\Lambda$ , and  $\bar{\Lambda}$  [6], as measured in central collisions of  $^{32}\text{S}$  with S at 200 GeV/nucleon by the NA35 Collaboration at CERN with a streamer chamber.

For our selection we have the following reasons.

(1) The high beam energy at CERN separates kinematically the central reaction zone around rapidity  $y_{c.m.} = 3$  from the fragmentation regions of the target and projectile at  $y = 0$  and  $y = 6$ . At BNL the span between target and projectile is smaller ( $y_{\text{proj}} - y_{\text{lab}} = 3.4$ ), and the width of each of the fragmentation regions  $\Delta y \approx 1-2$  leads to a mixing of all zones.

(2) The higher energies at CERN also generate a stronger longitudinal expansion of the matter, requiring at least cylindrical symmetry for the model, which we will introduce in the next section, to describe the data. The BNL data for the pions [7] are closer to an isotropic momentum distribution and might be described well by a spherically symmetric model as we have presented one already some time ago [8].

(3) The streamer chamber from NA35 provides for a large number of measurements in the same experiment and thus guarantees easy comparability. In this paper we will analyze the spectra of pions, protons,  $K_s^0$ ,  $\Lambda$ , and  $\bar{\Lambda}$ , which form the bulk of the hadronic matter.

(4) The symmetric collision system S+S together with

the selection of the events with 2% of the highest multiplicities minimizes the number of spectator nucleons, which did not collide with other nucleons at all. We are not interested in these nucleons, because they are similar to the majority of the nucleons in  $pA$  collisions, which suffer only a small energy or momentum transfer each. We are mainly interested in the participant nucleons, which generate the highest-energy densities and where we can expect the strongest collective effects and would look for a quark gluon plasma.

(5) The kinematic symmetry is experimentally fortunate, because only the wider open, easier accessible rear half of phase space ( $y \leq 3$ ) has to be measured, the other half can be obtained by reflection around  $y = 3$ . For example, by measuring the negative hadrons in the interval  $0.8 < y < 3.0$  and reflecting around  $y = 3$ , NA35 covers almost the whole rapidity gap between projectile and target. Also the isospin symmetry of  $^{32}\text{S}$  can be employed for the equality of proton and neutron spectra, as well as  $\pi^-$ ,  $\pi^0$ , and  $\pi^+$ , allowing for a determination of the proton spectra by subtracting the spectra of negative tracks from the spectra of the positive tracks with only a small error introduced by the possible inequality of the  $K^+$  and  $K^-$  spectra and  $\bar{p}$  contributions [5].

These advantages outweigh the disadvantage that S+S is not the biggest possible collision system to date. It contains with full overlap at most 64 nucleons, whereas a bigger target, e.g.,  $^{197}\text{Au}$ , would increase the number of participating nucleons to 115 in a simple geometric picture and moreover would raise the baryon and energy densities as well. However, besides the blurring of the theoretical explanation by the big number of non-participating nucleons, for an asymmetric collision system the phase space also has to be measured in a forward direction, which is experimentally increasingly difficult for the heavier collision systems. These data are thus not available yet,  $^{32}\text{S} + (^{107}/^{109})\text{Ag}$  is in analysis right now [11]. The biggest asymmetric system with a complete set of published hadron data is up to now  $^{16}\text{O} + ^{197}\text{Au}$  with a maximum number of participants ( $\sim 70$  from geometry) again similar to S+S.

Since the fundamental dynamics of an ultrarelativistic heavy ion reaction will basically be determined by strong interactions, the regular hadrons (pions, protons, and kaons) carry the major part of the total energy [12]. These particles spectra are most important for the global picture of the reaction. To a large extent we will rely on the pion spectra, because the pions are by number and also by energy (2/3 of total) the most important group and can be measured best, i.e., NA35 determines the  $\pi^-$  spectra by recording all negative tracks and only correcting them for electron tracks. The contamination by other particle species, i.e., by antiprotons or  $K^-$ , is quantitatively small and can be accounted for on a statistical basis.

In this paper we will only be interested in the *shape* of the spectra. The absolute multiplicities or the particle ratios convey little direct information about the reaction dynamics and require additional knowledge about the volume of the interaction zone or the equation of state, respectively. We will defer these questions to the

more detailed hydrodynamical simulation of the collision zone in [3].

### III. SPECTRA FROM A STATIONARY THERMAL SOURCE

#### A. A purely thermal source

In order to clarify the notation we start with the invariant momentum spectrum of particles radiated by a thermal source with temperature  $T$ :

$$E \frac{d^3n}{d^3p} = \frac{dn}{dy m_T dm_T d\phi} = \frac{gV}{(2\pi)^3} E e^{-(E-\mu)/T}, \quad (1)$$

where  $g$  is the spin-isospin-degeneracy factor for the particle species and  $\mu$  the grand canonical potential  $\mu = b\mu_b + s\mu_s$  as originating from its baryon and strangeness quantum numbers  $b$  and  $s$ . For simplicity we neglect quantum statistics with the reasoning that its influence will be rather small at the low densities where the particles typically decouple from each other and where the spectra are computed. This also holds true for the pions, whose Bose character is only then important for the spectral shape when chemical potentials close to the pion mass are introduced [13] via nonequilibrium arguments, which are somewhat beyond the scope of our analysis.  $V$  is the volume of the source, giving together with the factor  $e^{\mu/T}$  the normalization of the spectrum, which we will always adjust for a best fit to the data, because we are only interested in the *shape* of the spectra to reveal the dynamics of the collision zone at freeze out. In the remainder of the text we will always give the spectra in terms of rapidity  $y = \tanh^{-1}(p_L/E)$  and transverse mass  $m_T = \sqrt{m^2 + p_T^2}$ . Also  $\hbar = c = k_B = 1$ .

We obtain the transverse mass spectrum  $dn/(m_T dm_T)$  by integrating over rapidity using the modified Bessel function  $K_1$ , which behaves asymptotically like a decreasing exponential:

$$\frac{dn}{m_T dm_T} = \frac{V}{2\pi^2} m_T K_1\left(\frac{m_T}{T}\right) \xrightarrow{m_T \gg T} V' \sqrt{m_T} e^{-m_T/T}. \quad (2)$$

While the basic characteristics of the measured  $m_T$  spectra is indeed the exponential decay over several orders of magnitude with an almost uniform slope  $1/T$  when plotted over  $m_T$ , the  $\pi^-$  spectrum from NA35 shows a significant concave curvature (Fig. 1) on top of the exponential dropoff, which is not visible in the  $m_T$  spectra of the other particles ( $p$ ,  $K_s^0$ ,  $\Lambda$ ,  $\bar{\Lambda}$ ). This curvature makes it impossible for a single thermal source to fit both the low- and the high- $m_T$  region at the same time. (It does not stem from the curvature of the  $K_1$  function, since that one is much smaller and in the opposite direction.) The effect has been known under the name "*low- $m_T$  enhancement*" since the first data from the ultrarelativistic heavy ion experiments became available [4], and has stimulated many theoretical interpretations (for an overview see, e.g., [14]).

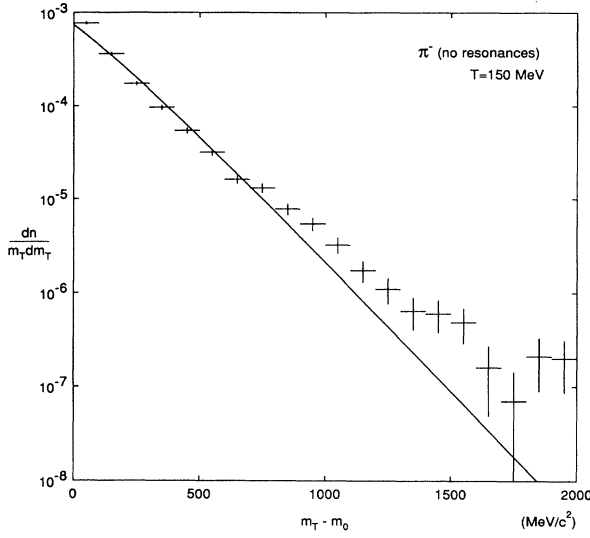


FIG. 1. Purely thermal  $\pi^-$   $m_T$  spectrum in comparison with data from NA35 S+S 200 A GeV [5]. A fit of a purely thermal source [Eq. (2)] was attempted to the data with temperature  $T$  as a free parameter. The absolute normalization was adjusted as best possible, nevertheless the deviations at medium and high  $m_T$  are significant.

Before we will devote ourselves to that problem in detail we finish the discussion of the thermal source with the rapidity distribution, which results from integrating the invariant momentum spectrum over the transverse components:

$$\frac{dn_{\text{th}}}{dy} = \frac{V}{(2\pi)^2} T^3 \left( \frac{m^2}{T^2} + \frac{m}{T} \frac{2}{\cosh y} + \frac{2}{\cosh^2 y} \right) \times \exp\left(-\frac{m}{T} \cosh y\right), \quad (3)$$

which reduces for light particles to  $dn/dy \propto \cosh^{-2}(y - y_0)$  up to third order in  $m/T$ . This rephrases the fact that the rapidity distribution of massless particles from an isotropic source is always the same regardless of their momentum dependence (e.g., [7]). Its full width at half height  $\Gamma_{\text{th}}^{\text{FWHM}} \approx 1.76$  is in sharp contrast to the experimental value for the pions of  $\Gamma_{\text{expt}}^{\text{FWHM}} = 3.3 \pm 0.1$  [5] (see dotted line in Fig. 4). The particle mass further narrows the rapidity distributions, leading for  $m > T$  to an additional Gaussian with the width parameter  $\sigma^2 = m/T$ , and increases the deviations from the measured distributions. Clearly here improvements are also necessary, which we will attempt in Sec. IV.

## B. Resonance decays

The attitude of the previous section was a bit too naive: Apart from the directly emitted pions of assumedly thermal origin the detector also detects pions, which originate from the decay of resonances, which are also generated in the reaction, e.g.,

$$\rho^0 \rightarrow \pi^+ \pi^-, \quad \omega \rightarrow \pi^+ \pi^0 \pi^-, \quad \text{or} \quad \Delta \rightarrow N \pi^-$$

and which have a very different spectral shape, thus distorting the straight exponential dropoff.

The abundant production of these resonances is an experimental fact, which has been investigated closely in  $pp$  collisions [15], where because of the much lower multiplicities the individual resonances can be reconstructed. Using these data as a guidance for our implementation in nucleus-nucleus collisions, we find that the absolute multiplicities of the resonances are distributed like  $\propto \exp(-m_R/T)$  with  $T \approx 180$  MeV, justifying a thermal description as an approximation as long as the temperature is close to this value. For the baryonic resonances ( $\Delta, \Lambda^*, \dots$ ) we also fix the baryon chemical potential to be  $\mu_B = 200$  MeV and distribute the strange resonances ( $K^*, \Lambda^*, \dots$ ) according to strangeness neutrality [16]. The spectral shape for the resonances has also been shown in  $pp$  experiments to be exponential with  $T \approx 180$  MeV and can for the heavy ion collisions quite safely be assumed to be thermal since frequent elastic collisions will equilibrate the resonances in the same way as the ground-state particles.

The decays of the heavier resonances into their lighter daughter particles has been investigated in detail by Sollfrank *et al.* in [17] and others [18]. Since we will analyze the mechanism in detail later in Appendix B, we will here only sketch the method of computation. The spectrum of the daughter particles is obtained by integrating the momentum distribution of the resonances with a factor  $f(W, p_R, p)$  describing the decay phase space [17] within the kinematic limits of invariant mass  $W$ , rapidity  $y$ , and transverse mass  $m_T$ :

$$\frac{d^2 n}{dy m_T dm_T} = \int_{W^{(-)2}}^{W^{(+)2}} dW^2 \int_{y_R^{(-)}}^{y_R^{(+)}} dy_R \int_{m_{TR}^{2(-)}}^{m_{TR}^{2(+)}} dm_{TR}^2 \times f(W, p_R, p) \frac{d^2 n_R}{dy_R m_{TR} dm_{TR}}. \quad (4)$$

To compute the  $\pi^-$  spectrum we evaluate (4) for the two-body decays  $\rho, K^{*-}, K^{0*}, \Delta, \Sigma^{*-}, \Sigma^{0*}, \Lambda^*$  as well as for the three-body decays of  $\omega$  and  $\eta$  numerically.

With these assumptions the transverse mass spectrum of the pions is again only a function of the temperature  $T$  and baryon chemical potential  $\mu_b$  and one can try a fit to the data. As shown in Fig. 2, we now succeed in reproducing the spectrum over the whole range in  $m_T$ , with the temperature  $T$  corresponding to the slope at high  $m_T$ . The kinematics of the resonance decays result in very steeply dropping daughter pion spectra and raise considerably the total pion yield at low  $m_T$ . For the heavier  $K_s^0, p, \Lambda$ , and  $\bar{\Lambda}$  (Fig. 3) the change in the spectra is less pronounced, since the mass difference between the resonance and the ground state is much smaller. Quite remarkably, we realize that all independent fits to these five particle spectra seem to agree in  $T \approx 200$  MeV within their statistical uncertainties [12,19].

We conclude that the resonance decays, as a necessary ingredient for any thermal model, already provide a good description of all measured hadronic  $m_T$  spectra. The magnitude of the effect (2/3 of the pions come from resonances) as it was assumed here, is caused by

the high fit temperature and has not been confirmed by further data, e.g., on the relative multiplicities of  $\rho$ ,  $\omega$ ,  $\Delta$ , etc., in S+S, so that there is still some room for other explanations (which should, however, always also take the resonances into account, albeit perhaps at a somewhat reduced level).

Especially the possibility of a chemical potential for the pions in size of  $\mu_\pi \approx 118$  MeV at  $T = 164$  MeV has been discussed [13], which might originate from non-equilibrium effects and which would accumulate pions at low momenta because of the nearby divergence of the Bose distribution. With our treatment of the  $\pi^-$  spectra we cannot exclude this effect, but we can reduce its importance by first subtracting the always present resonance contributions. In a quantitative analysis of the pion multiplicity in our hydrodynamic model [3], we determine that the nonequilibrium population of pions and the accompanying pion potential is much smaller than the pion mass and cannot influence the shape of the  $m_T$  spectra via the upwards curvature of the Bose distribution.

For a further overview of the low- $m_T$  enhancement we would like to refer to [14]. From our side the possibility of transverse flow was brought into the discussion with a model based on spherical symmetry [8]. Here, however, we will adopt cylindrical symmetry and analyze the longitudinal and transverse flows separately. While the longitudinal flow can be extracted from the data, the same uniqueness cannot be achieved for the transverse flow, though consistency arguments suggest its existence.

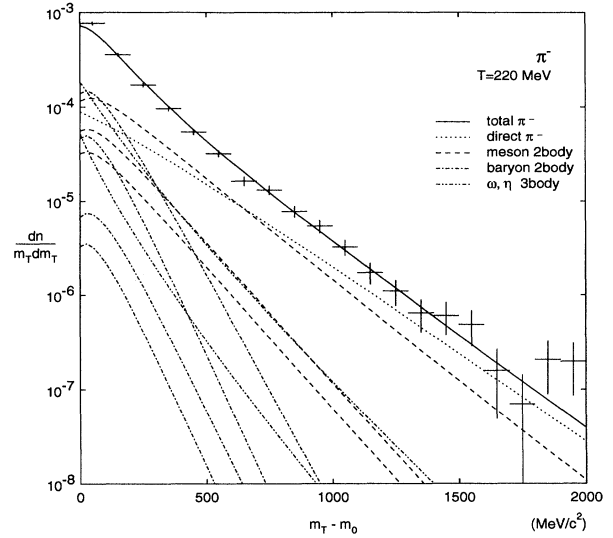


FIG. 2. Thermal  $\pi^-$   $m_T$  spectrum with resonance decays in comparison to data from NA35 S+S 200A GeV [5]. The purely thermal  $\pi^-$  and the two- and three-body decays of mesons and baryons add up to the total spectrum. The fit of the total  $\pi^-$  spectrum from a thermal source with the temperature  $T$  as a free parameter is very good over the full range. The absolute normalization has been adjusted for a best fit,  $\mu_b = 200$  MeV has been fixed. These results from [17] are repeated here for later comparison within a coherent presentation.

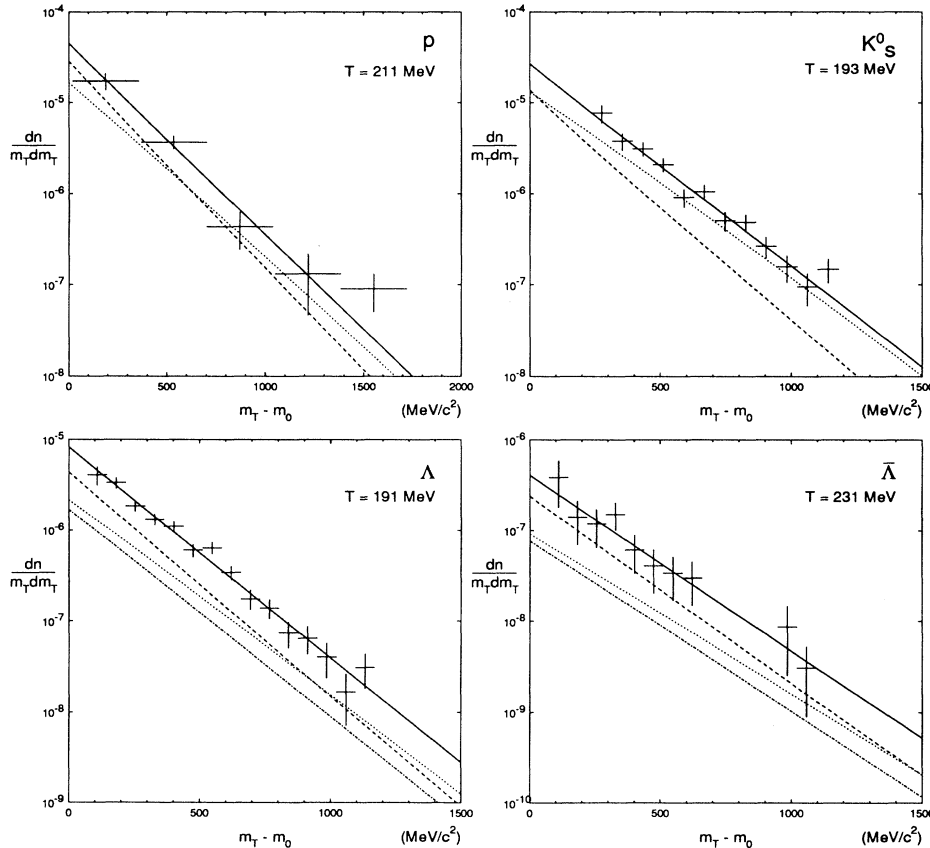


FIG. 3. Thermal  $m_T$  spectra of  $p$ ,  $K_S^0$ ,  $\Lambda$ , and  $\bar{\Lambda}$  including resonance decays in comparison with data from NA35 S+S 200 GeV/nucleon [5,6]. The purely thermal spectra (dotted) and the resonance decays (dashed) add up to the total spectra (solid). The respective fits to the  $m_T$  spectra are all very good and give similar temperatures. The absolute normalizations have been adjusted for a best fit,  $\mu_b = 200$  MeV has been fixed. These results from [17] are repeated here for later comparison within a coherent presentation.

## IV. SPECTRA FROM FLOWING SOURCES

### A. Longitudinal flow

We have already mentioned that the rapidity distribution of  $\pi^-$  (actually negatively charged hadrons) as measured by NA35 is much wider than a stationary thermal source could possibly predict. Also the inclusion of resonance decays does not improve this picture, since in the same way as they lead to a steepening of the  $m_T$  spectra at low  $m_T$  they cause a slight narrowing of the  $y$  distribution.

Obviously the momentum distribution of the measured pions is not isotropic, it rather has imprinted on it the direction of the colliding nuclei. The *boost-invariant* longitudinal expansion model, as it has been postulated by Bjorken [20] can explain such an anisotropy already at the level of particle production, which subsequently, after sufficient rescattering, leads to a boost-invariant longitudinal flow of matter with locally thermalized distributions. The observed particle spectrum then results from the summation of the spectra of individual thermal sources which are uniformly distributed in flow angle  $\eta$ . However, since the model has been formulated for asymptotically high energies, where the rapidity distribution of the produced particles establishes a plateau at midrapidity, we cannot apply it directly to our current energies, where already half of the total rapidity gap of 6 units is eaten up by the target and projectile fragmentation regions and consequently the pion distribution rather looks like a Gaussian.

We modify the boost-invariant scenario to account for the limited available beam energy by restricting the boost angle  $\eta$  to the interval  $(\eta_{\min}, \eta_{\max})$  [21]. The rapidity distribution is then the integral over the uniformly distributed thermal sources (3) boosted individually by  $\eta$ :

$$\frac{dn}{dy}(y) = \int_{\eta_{\min}}^{\eta_{\max}} d\eta \frac{dn_{\text{th}}}{dy}(y - \eta). \quad (5)$$

The transverse mass spectrum is not affected by this operation.

We can now try a fit of (5) to the measured  $\pi^-$   $y$  spectrum using  $\eta_{\max} = -\eta_{\min}$  as the single free parameter, because the distributions are not very sensitive to  $T$ . The rapidity distribution of negative hadrons from NA35 is measured over a large acceptance region ( $0 < p_T < 2 \text{ GeV}/c$ ) and can be identified with  $\pi^-$ , since the additional contributions from  $K^-$  and  $\bar{p}$  are small (5–10%) and probably distributed more or less homogeneously over the whole region [5]. The data points in the inaccessible region of the streamer chamber above  $y > 3.4$  can be substituted using symmetry with respect to  $y = 3$ .

We see in Fig. 4 that  $\eta_{\max} = 1.7$  fits the measured  $\pi^-$  spectra quite nicely. Again, the inclusion of the resonance decays does not qualitatively change the  $\pi^-$  distribution since the resonances are uniformly distributed over the boost rapidity  $\eta$  and thus have the same minor effect on integral (5) as they have on the individual thermal spectra (3). This would be different for inhomogeneities in the

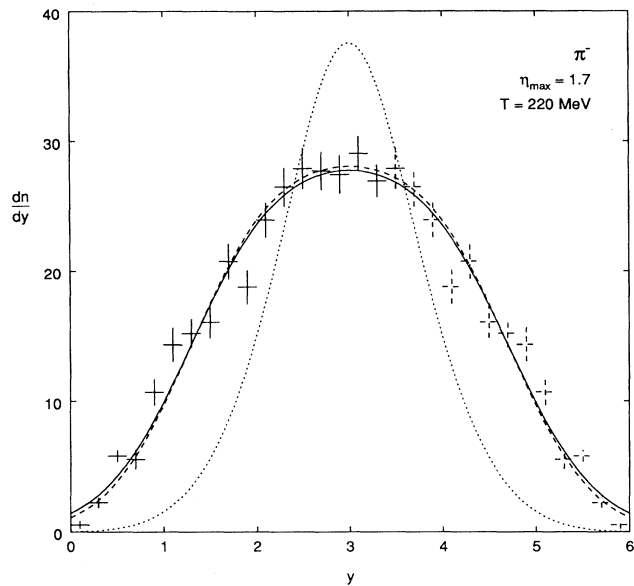


FIG. 4.  $\pi^-$   $y$  spectrum with longitudinal flow in comparison with data from NA35 S+S 200 A GeV [5], which have been reflected around  $y = 3$ . The maximal fluid rapidity  $\eta_{\max} = 1.7$  has been obtained from a fit of Eq. (5) to the measured spectrum. The absolute normalization has been adjusted for a best fit, the agreement with the data is very good. The temperature  $T = 220 \text{ MeV}$  has been taken from the fit to the  $m_T$  spectrum and has only a negligible influence on the  $y$  spectrum, similar to the inclusion of resonance decays (dashed line). For comparison also the purely thermal spectrum without any longitudinal flow is shown as a dotted curve.

resonance distributions: for example, a high concentration of  $\Delta$ 's in the fragmentation regions would manifest itself by additional pions from that region, i.e., bumps in the rapidity distribution [19].

Looking at the other hadronic distributions (Fig. 5), we see our interpretation basically confirmed. However, the experimental proton spectrum is much broader than the computed one and has a dip at central rapidity; the measured protons obviously carry still a big amount (50%) of their initial collision energy [12], and the spectrum contains many protons near the target and projectile fragmentation regions, which have not suffered sufficiently to have become part of the central fireball. Because there is no clearcut separation between the central region and the fragmentation regions in the experimental  $y$  spectrum, our model, which is crafted for the central region only, is bound to fail for the fragmentation zone protons.

The produced strange particles are much better reproduced: the theoretical  $K_s^0$  spectrum is only slightly too broad, the one for  $\Lambda$ 's slightly too narrow and the one for  $\bar{\Lambda}$ 's still satisfactory with the exception of the central data point which also has the largest statistical uncertainty. The strange particles are good indicators for collective flow, because all are produced particles which were absent in the original nuclei and are thus not con-

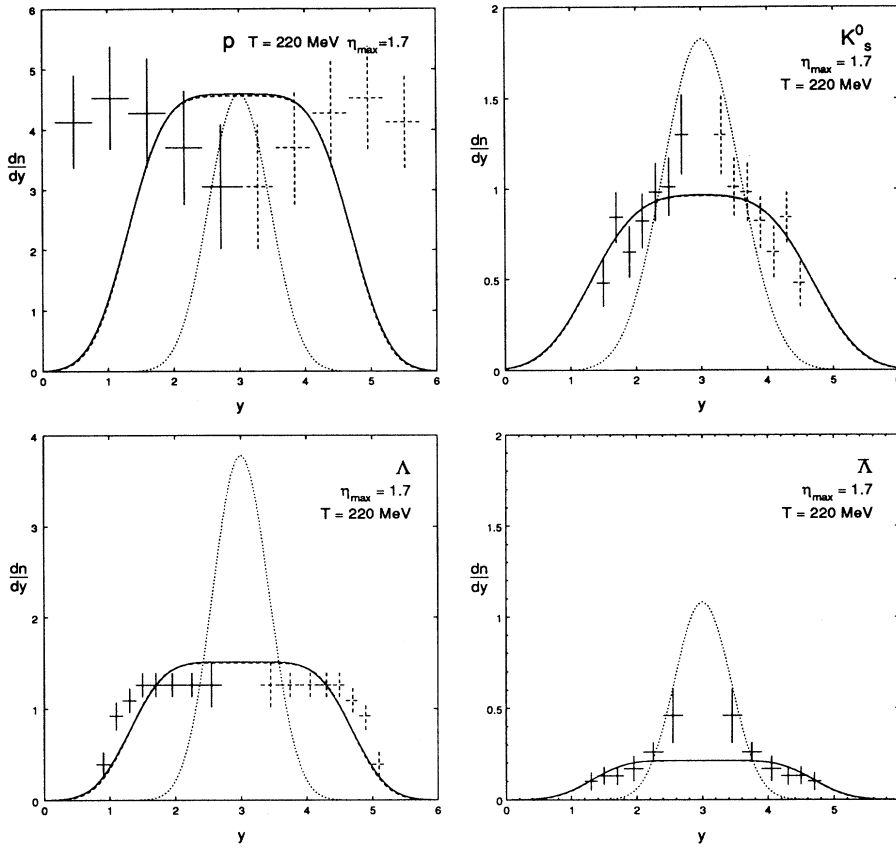


FIG. 5.  $y$  spectra of  $p$ ,  $K_s^0$ ,  $\Lambda$ , and  $\bar{\Lambda}$  with longitudinal flow in comparison with data from NA35 S+S 200 A GeV [5,6]. The flow  $\eta_{\max} = 1.7$  seen in the pions (Fig. 4) describes all produced spectra satisfactorily, only the protons still carry a large fraction of their initial collision energy. The absolute normalization was always adjusted for a best fit, the temperature and the resonance decays (dashed) have no influence on the spectra. For comparison also the purely thermal spectra without longitudinal flow are shown as dotted curves.

taminated by a cold spectator component at leading rapidities as the protons are. Also because of their bigger mass their flow component is more accentuated against the random thermal motion as in the case of the pions. Moreover, the disappearance of the characteristic polarization of the  $\Lambda$  [6] hints towards at least one other collision in the medium, which justifies viewing them as part of a thermalized system. For  $\bar{\Lambda}$  the situation is more complicated and the success of our model might be only accidental. We can imagine that they are produced centrally in particularly hard individual nucleon-nucleon collisions and have not yet approached thermal and chemical equilibrium between annihilation and production. We could thus expect to see in the  $\bar{\Lambda}$  distribution besides the flow component the imprint of the production process at central rapidities. However, a recent chemical analysis of the various particle ratios [22], which views the  $\bar{\Lambda}$ 's as an integral part of a thermally and chemically equilibrated fireball appears to be phenomenologically very successful and in favor of a thermalized picture which has already lost its memory of the production process.

We can also try a best fit of the hadronic  $y$  spectra individually by adjusting  $\eta_{\max}$  for each particle species separately (Fig. 6). Again we arrive at the same value of  $\eta_{\max} = 1.7 \pm 0.3$  independent of the temperature. Unfortunately, the  $y$  distributions of the heavier particles have less statistics than the pion spectrum and do not extend to as small rapidities; hence the estimates of the

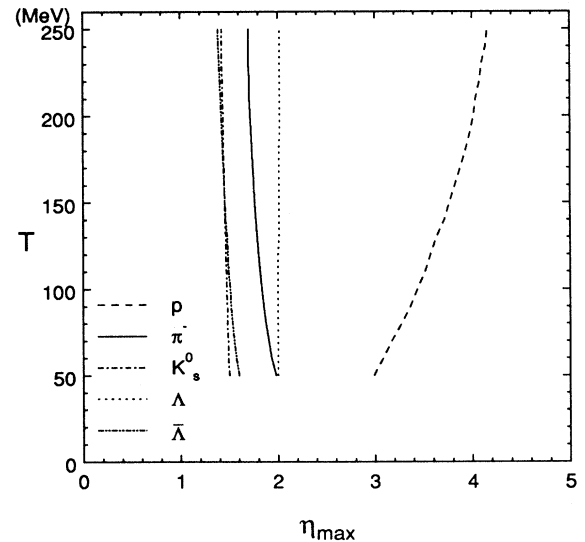


FIG. 6. The longitudinal flow  $\eta_{\max}$  can be extracted from the rapidity distributions of the hadrons. With the exception of the protons, which still carry a large fraction of their initial beam motion, a fit with  $\eta_{\max}$  as a free parameter gives for all produced particles independent of the assumed temperature a longitudinal flow similar to the pions with  $\eta_{\max} \approx 1.7$  at  $T \approx 200$  MeV.

widths rely heavily on the last data points. Therefore we will prefer to continue our reasoning with the better determined pion value.

### B. Transverse flow

The stepwise extension of the initial stationary thermal model by including resonance decays and a longitudinal flow component has provided a phenomenological description of almost all spectra— $dn/dy$  as well as  $dn/dm_T^2$ —of pions, protons,  $K_s^0$ ,  $\Lambda$ , and  $\bar{\Lambda}$  as measured in the experiment NA35. The few existing exceptions can be explained, they show the limits of our model. However, this seemingly complete picture of the dynamics of the hadronic matter has some serious intrinsic theoretical problems.

(1) On the one hand, at temperatures around 200 MeV the mean free path of pions in hadronic matter is much less than 1 fm, as we can estimate from the thermal distributions and averaged cross section of pions with nucleons and with each other [17]. On the other hand the size and lifetime of the reaction region is several fm, as can be guessed from the radius of the  $^{32}\text{S}$  nucleus and causality. The length of the collision zone will be even larger because the large time dilatation factors of the relativistic longitudinal expansion stretch the system quite long already during the formation time  $\tau_f \approx 1 \text{ fm}/c$ . Consequently, the pions cannot leave the interaction zone at  $T \approx 200 \text{ MeV}$  without further collisions, the reaction region cannot decouple thermally and should by continuing expansion force the pions to cool down further.

(2) The longitudinal expansion in the boost-invariant scenario corresponds to a solution of the hydrodynamical equations in (1+1) dimensions. In fact the one-dimensional expansion presumably dominates initially because of the anisotropic initial conditions. But it is inconsistent to assume that a thermalized system expands collectively in longitudinal direction without generating also transverse flow from the high pressures in the hydrodynamic system. This should be computed by hydrodynamics in at least 2+1 dimensions, if azimuthal symmetry is maintained, otherwise 3+1 dimensions, because the transverse expansion will increase the cooling rate.

(3) Already transverse velocities of about 0.3–0.6 $c$ , which are moderate compared to the longitudinal expansion with  $\beta_L = \tanh \eta_{\text{max}} > 0.9c$ , could change the transverse mass spectra considerably by enhancing the particle yields at high  $m_T$ .

We want to address these problems with a model which contains resonance decays and both longitudinal and transverse flow in order to put the discussion of the longitudinal and transverse spectra on a common basis. In this paper we will analyze how much information can be extracted from the data with such a model. Using our phenomenological analysis presented here we will extend in the next step [2,3] the model towards a global hydrodynamical description which enforces the mentioned theoretical consistency requirements. We observe (similar to [19]) that agreement with all the presented data can again be achieved and we prove the existence of transverse flow by theoretical means [2,3].

Not only theoretical necessities suggest the inclusion of transverse flow. There are further arguments for the actual existence of the phenomenon.

(1) At the lower BEVALAC energies ( $E/A \leq 2 \text{ GeV}$ ) a sideways flow of nuclear matter is observed [23]. It is generated by the squeeze out of nuclear matter in the collision and has been predicted by hydrodynamic computations [24]. Though this directed flow is of different nature from our collective expansion flow, it suggests the relevance of hydrodynamics also at higher energies.

(2) In a simple picture the transverse flow flattens, in the region  $p_\perp \lesssim m$ , the transverse mass spectra of the heavier particles more than for the lighter particles [25,8]. The AGS data [26] show clearly this tendency for pions, kaons, and protons.

(3) Event generators for nucleus-nucleus collisions show a statistical effect which can be interpreted as transverse flow. The statistical averaging of the velocities of many particles in a small volume can exhibit the transverse flow at AGS energies [27]. The VENUS event generator for nucleus-nucleus collisions shows also for CERN energies an increase of the spectra at high  $m_T$ , once the produced particles are allowed to rescatter [28]. The same effect is produced in our model by the transverse flow.

On the other hand we have to admit that from phenomenology alone there is no need for an additional transverse flow effect, since all the data have already been described nicely. Currently we thus will not be able to prove the existence of transverse flow from the data alone, only an indirect proof based on the phenomenological analysis together with hydrodynamical calculations with a consistent theoretical treatment of the freeze out process can be given [2]. But in the near future bigger collision systems can be expected with the Au beam at the AGS and with the installation of the Pb injector at CERN, which will lead to an increase of the collective effects. If we are currently not able to prove transverse flow directly from the data, the chances will be improving tomorrow, and we should develop our tools in the meantime.

We compute the spectrum by boosting the thermal sources now both in longitudinal and transverse direction. We describe the transverse velocity distribution  $\beta_r(r)$  in the region  $0 \leq r \leq R$  by a self-similar profile, which is parametrized by the surface velocity  $\beta_s$ :

$$\beta_r(r) = \beta_s \left( \frac{r}{R} \right)^n . \quad (6)$$

With  $n$  we can vary the form of the profile. We choose customarily  $n = 2$ , because the quadratic profile resembles the solutions of hydrodynamics closest [1]. Anyway, the form of the profile is not important for the analysis, as we checked with the case  $n = 1$ . Leaving the details of the computation to Appendix A, the resulting spectrum is a superposition of the individual thermal components, each boosted with the boost angle  $\rho = \tanh^{-1} \beta_r$ :

$$\frac{dn}{m_T dm_T} \propto \int_0^R r dr m_T I_0 \left( \frac{p_T \sinh \rho}{T} \right) K_1 \left( \frac{m_T \cosh \rho}{T} \right) . \quad (7)$$

From Figs. 7 and 8 we see that also with a moderate transverse flow ( $\beta_s = 0.5c$ , i.e.,  $\langle\beta_r\rangle = 0.25c$ ) very good fits to all hadron spectra can be obtained, again treating the temperature as a free parameter. The temperature of the local sources as extracted from the data is again surprisingly uniform but now much smaller than without transverse flow (Figs. 2 and 3), thereby reducing the contribution from the resonances. A quantitative explanation of this effect will be given later in Appendix A, qualitatively the effect is similar to a blue shift as caused by a rapidly approaching source, shifting particles to higher momenta. The heavier the particles, the more they profit from the flow velocity.

We condense the information from the  $m_T$  spectra with respect to the transverse flow in Figs. 9 and 10 where we show all possible fit pairs ( $T, \beta_s$ ) for all hadronic spectra. Without transverse flow ( $\beta_s = 0$ ) the intercepts of the curves with the axis show the fitted temperatures of stationary thermal emitters including resonance decays (Figs. 2 and 3), where all temperatures cluster around the value  $T \approx 210 \pm 20$  MeV. Surprisingly, despite their somewhat different shapes, the curves stay together in one band and only weakly concentrate in the region  $\beta_s \approx 0.5c$ .

Intuitively one would rather expect the contrary: Because flow increases the particle energies according to their rest masses ( $\langle E \rangle \approx \langle E \rangle_{th} + \frac{m_0}{2} v_{coll}^2$ ), the heavier particles profit more from the collective motion than the lighter ones. Since both transverse flow and the local

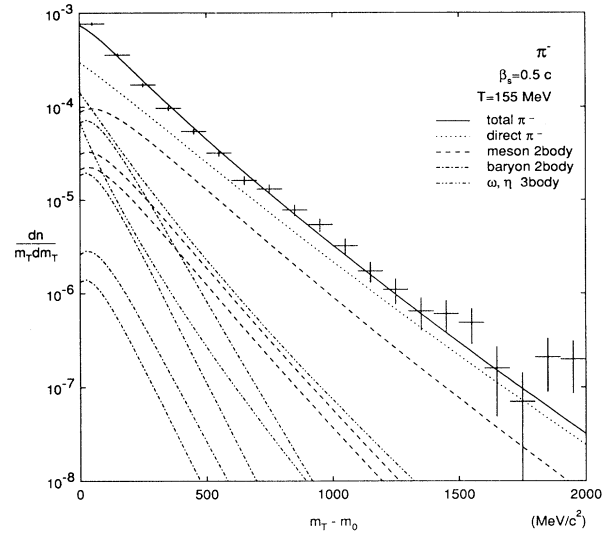


FIG. 7.  $\pi^-$   $m_T$  spectrum with resonance decays and transverse flow in comparison with data from NA35 S+S 200A GeV [5]. The total  $\pi^-$  spectrum consists of the original pions and the decay pions. Based on a parabolic transverse velocity profile with  $\beta_s = 0.5c$  the fit with temperature  $T$  as the free parameter is quite good over the whole  $m_T$  range. The absolute normalization has been adjusted for a best fit,  $\mu_b = 200$  MeV has been fixed to allow for a moderate baryon population.

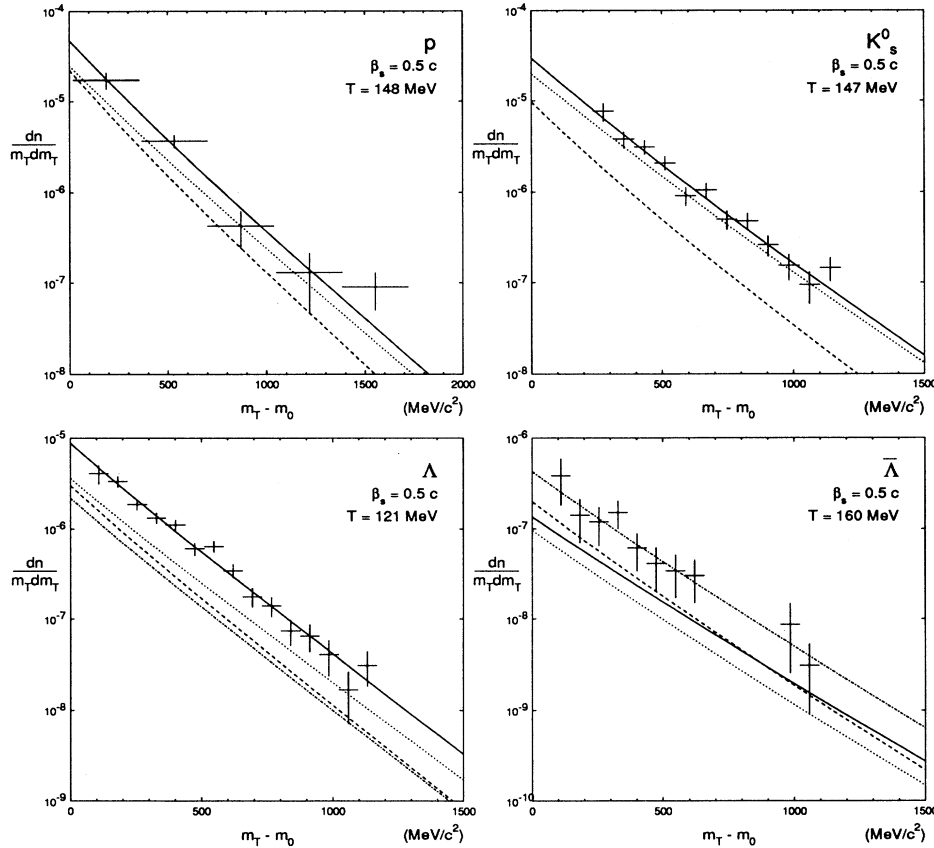


FIG. 8. The  $m_T$  spectra of  $p$ ,  $K_s^0$ ,  $\Lambda$ , and  $\bar{\Lambda}$  with decays and transverse flow in comparison with the data from NA35 S+S at 200A GeV [5,6]. Based on a parabolic transverse velocity profile with  $\beta_s = 0.5c$  the individual fits with the temperature as the free parameter show good agreement with the data at temperatures similar to Fig. 7. The absolute normalization has been adjusted for a best fit,  $\mu_b = 200$  MeV has been fixed as in Fig. 7.

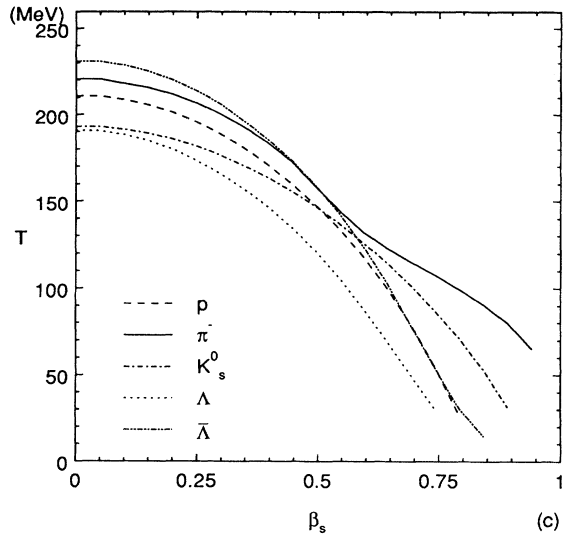


FIG. 9. All fitpairs  $(T, \beta_s)$  of the  $\pi^-$ ,  $K_s^0$ ,  $p$ ,  $\Lambda$ , and  $\bar{\Lambda}$   $m_T$  spectra. Every point on these curves gives good agreement of the computed  $m_T$  spectrum (with resonances and transverse flow) with the respective measured spectrum.

temperature determine the slope of the  $m_T$  spectrum, a bigger effect from flow for the heavier particles should result in faster dropping  $(T, \beta_s)$  curves from the fits for  $K_s^0$ ,  $p$ , and  $\Lambda$ . The different shapes of the curves should make it possible to find one unique intersection point, representing  $T$  and  $\beta_s$  of the collective system [8]. Unfortunately, this simple argument does not take the resonance decays into account, which modify especially the pion spectra strongly [17]. We show in Fig. 11 the curves, which unrealistically omit the resonance decays, and from which we would erroneously deduce a transverse flow of

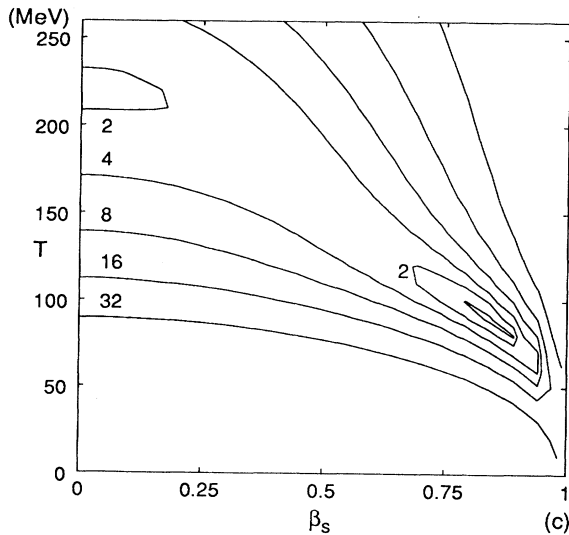


FIG. 10. Quality of the  $(T, \beta_s)$  fits for the  $\pi^-$   $m_T$  spectrum (Fig. 9). The contour lines designate the areas of  $\chi^2/NDF = 1, 2, 4, 8, 16,$  and  $32$ .  $\mu_b$  has been fixed at 200 MeV.

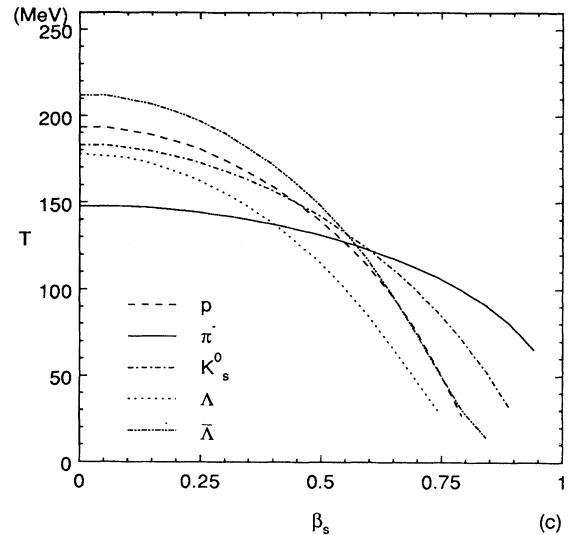


FIG. 11. Fit pairs of  $\pi^-$ ,  $K_s^0$ ,  $p$ ,  $\Lambda$ , and  $\bar{\Lambda}$   $m_T$  spectra omitting the decay contributions. In this unrealistic situation there would be an intersection around  $\beta_s \approx 0.5c$ , which would strongly favor a sizable transverse flow.

$\beta_s \approx 0.5c$  from the unique intersection of all curves. However, as we see in Fig. 9, reality is more complicated, the pion curve is considerably modified by resonance decays so that in the end its shape resembles the heavy particles and all values  $0 < \beta_s < 0.7c$  seem to be possible within the experimental uncertainties.

The  $\Lambda$  do not quite fit into the picture, they seem a bit colder than the other particles including the protons. An explanation in terms of an admixture of colder  $\Lambda$  from the fragmentation region is supported by the the rapidity distribution but is in some contradiction to the higher proton temperature (which however has experimentally the biggest error bars). In a similar manner one could justify the higher temperatures of  $\bar{\Lambda}$  which seem to originate more from the hotter center.

We can conclude that the data alone do not make a unique statement about the existence of transverse flow. Instead of a single point for  $\beta_s$  there is a band with many pairs  $(T, \beta_s)$ . The phenomenological analysis has fully exploited the available data and has to stop here. Which point on these curves corresponds to the freeze-out point of a consistent hydrodynamical evolution will be studied in a separate paper [2,3]. The theoretical methods presented there can use the gathered information to back-extrapolate towards the early stages of a heavy ion collision and to eventually fix the amount of transverse flow.

## V. DISCUSSION AND CONCLUSIONS

Naturally there is some doubt whether collective effects are actually as important as it might seem from the analysis presented here, since the  $S$  nucleus is still very small. Comparing  $S+S$  to  $pp$  minimum bias data, which should resemble most closely the average nucleon-nucleon

collision in S+S, we realize that the rapidity distributions are rather similar in shape. Accounting for the isospin symmetry, the width of the S+S distribution turns out to be only about 10% smaller than from  $pp$  [5,12].

The transverse momentum spectra show bigger differences when plotted as the (normalized) ratio of  $SS/pp$  [29]. Apparently there is an enhancement at low  $p_T$ , which could result from the increased population of resonances, and a significant enhancement at high  $p_T$ , which we would contribute to the bigger transverse flow. However, a high- $p_T$  enhancement has also been observed in  $pA$  collisions [30] (Cronin effect), although this effect sets in only above  $p_{\perp} \approx 1.5$  GeV. It has been interpreted as resulting from multiple collisions of the partons in the nucleus [31] and as such is a QCD specific effect. We interpret this multiple scattering already in  $pA$  as an indicator that collective matter flow can be generated, since in the limit of many scatterings hydrodynamic behavior will eventually result.

It would be too impulsive to deduce from the apparent similarity of  $pp$  and S+S spectra that the collective interpretation is wrong, since (a)  $pp$  is by no means an elementary collision system which we understand in sufficient detail to serve as the antipode of a collective system and (b) only a few of the observed features of the spectra can be fully reproduced by these two radically different philosophies which share only a small set of common principles as local energy-momentum conservation, relativistic space-time picture, etc. For other observables, which are not directly tied to the dynamics, e.g., strangeness, we already see a big enhancement compared to  $pp$ , thus indicating fundamental differences between both collision systems.

A careful systematic study of the  $A$  dependence from  $pp$  up to Pb+Pb should allow one to decide this question by showing the increasing importance of the collective effects for the bigger systems relative to the individual scattering processes. Unfortunately at the present time the only other symmetric collisions at high energies are  $pp$  collisions [32], because, as we already mentioned, we cannot directly compare with asymmetric ( $pA$ ) collisions. The data from the no longer operating ISR (intersecting storage rings) from light nuclei ( $dd$ ,  $\alpha\alpha$ ) [33] would also be very interesting, but they probably have to be reanalyzed for a direct comparison.

Nevertheless, from our experience with S+S we can already risk the prediction that the spectral shape from Pb+Pb collisions will show only gradual changes from S+S and that a careful analysis will be needed to uncover the interesting physics. How much influence the creation of a plasma would have on the spectra cannot be answered in this context without additional theory, but we would already like to caution big expectations, since the plasma would be created in the early stages of the collision and any signal would be leveled by the following hadronic stages with their own dynamics.

In conclusion we have shown that a thermal model is perfectly possible for S+S collisions despite (or because of) the similarity of S+S and  $pp$  spectra. The data force us to include resonance decays and longitudinal flow while they make no decisive statement about

the existence of transverse flow. But through further theoretical investigations the quantitative analysis presented here can be used to prove the existence of transverse flow and infer other informations about the collision zone [2,3].

## ACKNOWLEDGMENTS

We thank S. Wenig for supplying us with the charged particle data prior to publication. E.S. gratefully acknowledges support by the Deutsche Forschungsgemeinschaft (DFG), the Alexander von Humboldt Stiftung and the U.S. Department of Energy under Contract Nos. DE-AC02-76H00016 and DE-FG02-93ER40768. J.S. gratefully acknowledges support by a fellowship from the Free State of Bavaria and the DFG. U.H. gratefully acknowledges support by the DFG, the Bundesministerium für Forschung und Technologie (BMFT), and the Gesellschaft für Schwerionenforschung (GSI).

## APPENDIX A: SLOPES FROM TRANSVERSE FLOW

Both transverse flow and resonance decays have a strong impact on the  $m_T$  spectra. In this and the following appendix we will show the actual computation of the spectra, and we will try to disentangle both influences by analyzing the slope of the  $m_T$  spectrum.

We follow the spirit of the boost-invariant scenario by first defining the transverse velocity field in the central slice (using the boost angle  $\rho = \tanh^{-1} \beta_r$ ) for azimuthal symmetry

$$u'^{\nu}(\tilde{t}, r, z = 0) = (\cosh \rho, \vec{e}_r \sinh \rho, 0), \quad (A1)$$

and later boosting it in a longitudinal direction (boost angle  $\eta$ ) to generate the whole velocity field [34]

$$u^{\mu}(\rho, \eta) = (\cosh \rho \cosh \eta, \vec{e}_r \sinh \rho, \cosh \rho \sinh \eta). \quad (A2)$$

Note that  $u^{\mu}$  is not symmetric with respect to the boost angles  $\rho$  and  $\eta$ . This results from the fact that Lorentz transformations for different directions do not commute.

Having defined the velocity field, the invariant momentum spectrum is given by [35]

$$E \frac{d^3 n}{d^3 p} = \int_{\sigma} f(x, p) p^{\lambda} d\sigma_{\lambda} \\ \approx \frac{g}{(2\pi)^3} \int e^{-(u^{\nu} p_{\nu} - \mu)/T} p^{\lambda} d\sigma_{\lambda}, \quad (A3)$$

where  $f(x, p)$  is the invariant distribution function, which we assume to be an isotropic thermal distribution boosted by the local fluid velocity  $u^{\mu}$ , and we approximate the respective Bose and Fermi distributions by the Boltzmann distribution.

This mathematical formulation measures directly the

particle flow through the given hypersurface  $\sigma$  as if the virtual walls of the fluid cells have suddenly disappeared and the particles are flying isotropically in all directions.  $\sigma$  should not be visualized as a real surface which emits radiation only to the outside. Instead it defines the borderline between hydrodynamical behavior and free-streaming particles, which are both idealizations, as a mathematical construct. More intuitive approaches lead to formulas [36] which no longer obey the conservation laws. In reality the freeze-out hypersurface might be defined by the points of the last interaction of each individual particle and thus acquires a thickness of the order of the mean free path. This seems to be difficult to implement consistently with the dynamical evolution and for our purposes the simple model seems to be quite sufficient.

We parametrize the hypersurface  $\sigma(r, \phi, \zeta)$  in cylindrical coordinates  $0 \leq r \leq R$ ,  $0 \leq \phi < 2\pi$ , and  $-\eta_{\max} \leq \zeta \leq \eta_{\max}$  in longitudinal directions. We invoke

instantaneous freeze out in the  $r$  direction to keep matters simple, but allow for more general shapes  $[t(\zeta), z(\zeta)]$  in the longitudinal direction (e.g., hyperbolas [20]) because of the large longitudinal time dilatation effects:

$$\sigma^\mu(r, \phi, \zeta) = [t(\zeta), r \cos \phi, r \sin \phi, z(\zeta)], \quad (\text{A4})$$

$$p^\mu d\sigma_\mu = \left[ E \frac{\partial z}{\partial \zeta} - p_L \frac{\partial t}{\partial \zeta} \right] r dr d\phi d\zeta. \quad (\text{A5})$$

For the argument of the Boltzmann distribution we need the momentum of the particle in the center-of-fireball system

$$u^\mu p_\mu = m_T \cosh(y - \eta) \cosh \rho - p_T \sinh \rho \cos(\phi - \varphi). \quad (\text{A6})$$

Because of azimuthal symmetry we can integrate over  $\phi$  making use of the modified Bessel function  $I_0(z) = (2\pi)^{-1} \int_0^{2\pi} e^{z \cos \phi} d\phi$ :

$$E \frac{d^3 n}{d^3 p} = \frac{g}{(2\pi)^2} \int_{-\eta_{\max}}^{\eta_{\max}} d\zeta \left[ m_T \cosh y \frac{\partial z}{\partial \zeta} - m_T \sinh y \frac{\partial t}{\partial \zeta} \right] \int_0^R r dr \exp\left(-\frac{m_T \cosh \rho \cosh(y - \eta) - \mu}{T}\right) I_0\left(\frac{p_T \sinh \rho}{T}\right). \quad (\text{A7})$$

For the transverse mass spectrum we integrate with the help of another modified Bessel function  $K_1(z) = \int_0^\infty \cosh y e^{-z \cosh y} dy$ :

$$\begin{aligned} \frac{dn}{m_T dm_T} &= \frac{g}{\pi} m_T \int_{-\eta_{\max}}^{\eta_{\max}} d\zeta \left[ \cosh \eta \frac{\partial z}{\partial \zeta} - \sinh \eta \frac{\partial t}{\partial \zeta} \right] \int_0^R r dr K_1\left(\frac{m_T \cosh \rho}{T}\right) I_0\left(\frac{p_T \sinh \rho}{T}\right) \\ &= \frac{2g}{\pi} m_T Z_i \int_0^R r dr K_1\left(\frac{m_T \cosh \rho}{T}\right) I_0\left(\frac{p_T \sinh \rho}{T}\right). \end{aligned} \quad (\text{A8})$$

We see that the transverse mass spectrum factorizes, as long as temperature and transverse flow are independent of the longitudinal position in a longitudinally comoving coordinate system. There is only a factor  $Z_i$  affecting the normalization. The invariant momentum spectrum factorizes only for small transverse flows ( $\cosh \rho \approx 1$ ) into a longitudinal and a transverse part. The rapidity distribution is almost independent of transverse flows, even if the latter becomes large, as we have checked explicitly.

The general formula for azimuthal symmetry allowing noninstantaneous freeze out in the  $r$  direction ( $\partial t / \partial r \neq 0$ ) is rather similar, involving also  $K_0$  and  $I_1$ :

$$\begin{aligned} \frac{dn}{m_T dm_T} &= \frac{g}{\pi} \int_{-\eta_{\max}}^{\eta_{\max}} d\zeta \int_0^{R(\zeta)} r dr \left\{ \left[ \cosh \eta \frac{\partial z}{\partial \zeta} - \sinh \eta \frac{\partial(t, r)}{\partial(\zeta, r)} \right] m_T K_1\left(\frac{m_T \cosh \rho}{T}\right) I_0\left(\frac{p_T \sinh \rho}{T}\right) \right. \\ &\quad \left. - \frac{\partial z}{\partial \zeta} \frac{\partial t}{\partial r} p_T K_0\left(\frac{m_T \cosh \rho}{T}\right) I_1\left(\frac{p_T \sinh \rho}{T}\right) \right\}. \end{aligned} \quad (\text{A9})$$

We can achieve a better understanding of the transverse mass spectrum in (A8) by analyzing its slope. Fixing the variables  $r, \eta, T$  at reasonable values we focus on the  $m_T$  dependent parts. The slope in a semilogarithmic plot is

$$\begin{aligned} \frac{d}{dm_T} \ln\left(\frac{dn}{m_T dm_T}\right) &= \frac{d}{dm_T} \ln\left[m_T I_0\left(\frac{p_T \sinh \rho}{T}\right) K_1\left(\frac{m_T \cosh \rho}{T}\right)\right] \\ &= \frac{I_1\left(\frac{p_T \sinh \rho}{T}\right)}{I_0\left(\frac{p_T \sinh \rho}{T}\right)} \frac{m_T \sinh \rho}{p_T T} - \frac{K_0\left(\frac{m_T \cosh \rho}{T}\right) \cosh \rho}{K_1\left(\frac{m_T \cosh \rho}{T}\right) T}. \end{aligned} \quad (\text{A10})$$

We can immediately derive the limiting case for large  $m_T$ , since there  $m_T/p_T \rightarrow 1$ ,  $K_0/K_1 \rightarrow 1$ , and for finite flow ( $\sinh \rho > 0$ ) also  $I_1/I_0 \rightarrow 1$ :

$$\lim_{m_T \rightarrow \infty} \frac{d}{dm_T} \ln \left( \frac{dn}{m_T dm_T} \right) = \frac{\cosh \rho - \sinh \rho}{T} = -\frac{1}{T} \sqrt{\frac{1 - \beta_r}{1 + \beta_r}}. \quad (\text{A11})$$

The apparent temperature, understood as the inverse slope at high  $m_T$ , is then larger than the original temperature by a blue shift factor, see also [37]:

$$T_{\text{eff}} = T \sqrt{\frac{1 + \beta_r}{1 - \beta_r}}. \quad (\text{A12})$$

For small values of  $m_T$  the situation is much less clear, as one can see from Fig. 12. We cannot expect a simple expansion around  $m_T = \infty$  to deliver fully satisfying results, because apart from the shape of the Bessel functions also the particle mass  $m_0$  (via  $p_T = \sqrt{m_T^2 - m_0^2}$ ) and the fluid rapidity  $\rho$  influences the slope. Nevertheless, the basic tendency can be discussed with this expansion

$$\begin{aligned} \frac{d}{dm_T} \ln \left( \frac{dn}{m_T dm_T} \right) &\approx -\frac{\sinh \rho - \cosh \rho}{T} - \frac{m_0^2 \sinh \rho}{2m_T^2 T} \\ &+ \frac{3}{16} \frac{T}{m_T^2} \left( \frac{1}{\sinh \rho} + \frac{1}{\cosh \rho} \right). \end{aligned} \quad (\text{A13})$$

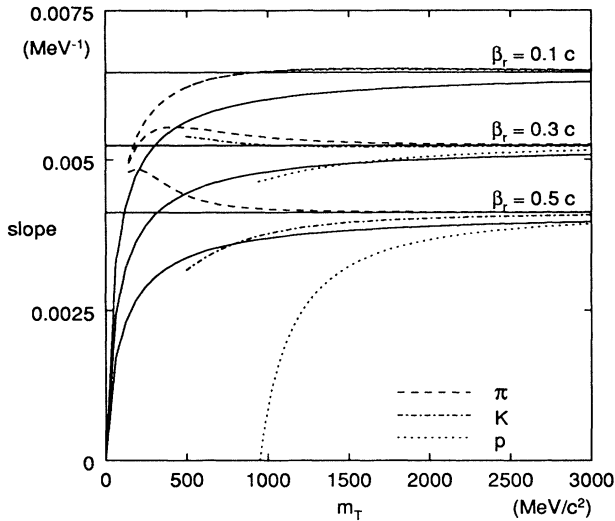


FIG. 12.  $m_T$  slopes with transverse flow for pions, kaons, and protons. Every group of curves corresponds to a fixed transverse expansion velocity  $\beta_r$ . The approximations of the curves by the pure exponentials (horizontal lines) are remarkably good already at low  $m_T$ . For comparison we included also the slopes of thermal sources (in Boltzmann statistics) with correspondingly blue shifted temperatures (solid curves). Compare also with Fig. 13.

The first term is again the blue shift factor, the additional terms are responsible for the curvature of the spectrum. The deviations from the exponential behavior are largest for large flows ( $\sinh \rho \gg 0$ ) and have the biggest effect at low  $m_T$ , where the shape of the Bessel functions tends to steepen the spectra, while big particle masses strongly flatten the spectrum there [8].

One can extract regions from the figure, where the slope approaches the limiting value satisfactorily. For pions and kaons we have  $m_T > 1000$  MeV, whereas for nucleons in the case of strong flow the limiting slope will be approached only above  $m_T > 2000$  MeV. This has to be contrasted with the behavior of the resonance decays which only affect the low  $m_T$  region (see Fig. 13).

Since in a realistic picture there are various components of transverse flow, we account for them by a superposition of simple exponentials, each with its own blue shift, denoted by  $b_r(\beta_r) = \sqrt{(1 - \beta_r)/(1 + \beta_r)}$ , to compute the blue shift factor of the integrated spectrum:

$$b_{\text{int}} = -T \frac{d}{dm_T} \ln \int_0^R \exp \left( -b_r(\beta_r) \frac{m_T}{T} \right) r dr. \quad (\text{A14})$$

The integrals could be solved analytically for  $n = 1$  and 2, but it is more instructive to expand them into a power series in  $1 - b_s$  under the assumption that  $m_T/T$  is not too big:

$$b_{\text{int}} \approx \begin{cases} 1 - \frac{1}{2}(1 - b_s) - \frac{(m_T/T)^{-3}}{12}(1 - b_s)^2 + \dots & (n = 2), \\ 1 - \frac{2}{3}(1 - b_s) - \frac{2(m_T/T)^{-5}}{36}(1 - b_s)^2 + \dots & (n = 1), \\ 1 - \frac{4}{5}(1 - b_s) - \frac{2(m_T/T)^{-3}}{75}(1 - b_s)^2 + \dots & (n = \frac{1}{2}), \\ 1 - (1 - b_s) & (n = 0), \end{cases} \quad (\text{A15})$$

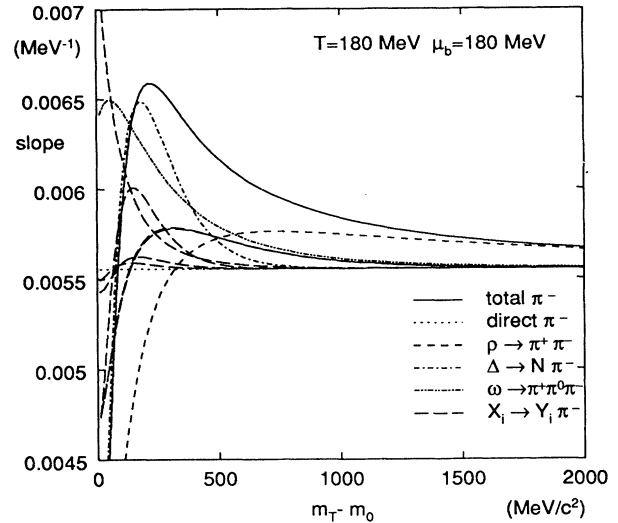


FIG. 13.  $m_T$  slopes of  $\pi^-$  with resonance decays. For realistic values of  $T$  and  $\mu_b$  we show the slopes resulting from the addition of always one resonance channel to the purely thermal  $\pi^-$  spectrum. At high  $m_T$  only the  $\rho$  decay changes the slope by a few percent. At lower  $m_T$  many individual contributions (especially  $\Delta$  and  $\omega$ ) add up to a significant modification of the total spectrum. Interesting is the comparison with Fig. 12 (scales are different).

where the terms in third order do not improve the approximation considerably. Approximating the blue shift factor to first order by  $b_s \approx 1 - \beta_s$ , we arrive at a surprising coincidence with the average fluid velocity

$$b_{\text{int}} \approx \sqrt{\frac{1 - \langle \beta_r \rangle}{1 + \langle \beta_r \rangle}} \approx 1 - \frac{2}{n+2} \beta_s, \quad (\text{A16})$$

which is a handy way to estimate the behavior of the fits in Fig. 9.

In conclusion we find from our simple quantitative estimates that the influence of the transverse flow on the transverse momentum spectrum is strong. We also investigated the influence of the geometry of the freeze-out hypersurface on both the  $y$  and  $m_T$  spectra. General formulas developed in [38,39] show that the shape of the hypersurfaces influences the spectra via the partial

derivatives of  $\sigma$  with respect to  $r$  and  $z$ . Similar to the spherical case [8] we have not encountered big differences in the width of the  $y$  spectra as well as the slope of the  $m_T$  spectra as long as we confined ourselves to realistic freeze-out hypersurfaces.

## APPENDIX B: SLOPES FROM RESONANCE DECAYS

Computing the spectrum of the resonance products is generally a complex task and requires a computer to do the phase space integrals numerically. However, investigating the simpler case of the two-body decay analytically can give us some insights into the resulting spectra. We start from the general formula in [17], now specialized for two-body decays:

$$\frac{d^2 n}{dy m_T dm_T} = \frac{m_R b}{4\pi p^*} \int_{y_R^{(-)}}^{y_R^{(+)}} \frac{dy_R}{\sqrt{m_T^2 \cosh^2(y - y_R) - p_T^2}} \int_{m_{TR}^{(-)}}^{m_{TR}^{(+)}} \frac{dm_{TR}^2}{\sqrt{(m_{TR}^{(+)} - m_{TR})(m_{TR} - m_{TR}^{(-)})}} \frac{d^2 n_R}{dy m_{TR} dm_{TR}}. \quad (\text{B1})$$

By introducing a thermal spectrum for the resonances which is independent of rapidity  $\frac{d^2 n}{dy m_T dm_T} = C_1 m_{TR} e^{-m_{TR}/T}$ , we can solve one further integral analytically:

$$\frac{d^3 n}{dy m_T dm_T} = \frac{m_R}{4\pi p^*} \int_{y_R^{(-)}}^{y_R^{(+)}} \frac{dy_R}{\sqrt{m_T^2 \cosh^2(y - y_R) - p_T^2}} \pi C_1 e^{-a/T} \left\{ 2(a^2 + b^2) I_0\left(\frac{b}{T}\right) - (4ab + 2Tb) I_1\left(\frac{b}{T}\right) \right\}. \quad (\text{B2})$$

where  $a = \frac{1}{2}(m_{TR}^{(+)} + m_{TR}^{(-)})$  and  $b = \frac{1}{2}(m_{TR}^{(+)} - m_{TR}^{(-)})$ . For large  $m_T$ ,  $a$  and  $b$  are approximately independent of  $y_R$ ,

$$a \approx \frac{m_R E^* m_T}{m^2} := \bar{a}, \quad b \approx \frac{m_R p^* p_T}{m^2} := \bar{b} \quad (\text{B3})$$

and we can extract in first order the slope of the transverse mass spectrum since the Bessel functions  $I_i(\bar{b}/T)$  behave asymptotically like exponentials  $\exp(\bar{b}/T)$ . The resulting exponential is  $\exp[(\bar{b} - \bar{a})/T]$  giving a slope at high  $m_T$ :

$$\frac{d}{dm_T} \ln \frac{dn}{m_T dm_T} \approx -\frac{m_R (E^* - p^*)}{m^2} \frac{1}{T}. \quad (\text{B4})$$

$E^*$  and  $p^*$  are the energy and momentum of the daughter particle in the rest system of the resonance and are for the two-body decay already given by the particle masses ( $p^*$  is listed for every decay channel in [40]). The estimate (B4) coincides very well with the slopes of the numerically computed spectra at large  $m_T$ .

Further approximations reveal for the slope  $\frac{m_R}{p^*} \frac{1}{T}$  or the effective temperature

$$T_{\text{eff}} \approx \frac{p^*}{m_R} T. \quad (\text{B5})$$

Since  $p^* < m_R$  the spectra of the daughter particles are

generally steeper than the original spectrum of the resonance, which translates into a lower apparent temperature of the pion spectra at low  $m_T$  (Fig. 13).

We can also estimate the width of the rapidity distribution by looking at the integration limits for  $y_R$ . The maximal rapidity difference between resonance and daughter particle is restricted by kinematics to

$$|y_R - y| \leq \sinh^{-1} \left( \frac{p^*}{m_T} \right). \quad (\text{B6})$$

For the  $\Delta$  decay  $p^* = 227$  MeV, so that the decay pion can move at most 1.27 units of rapidity (at  $m_T = m_0$ ), and the nucleon at most 0.24. The actual  $(y_R - y)$  distribution of the daughter particle will naturally be much smaller, as can be inferred from the width of an isotropic distribution, which is for massless particles  $\Gamma^{\text{FWHM}} = 2 \times 0.88$  [Eq. (3)]. This similarity to a thermal source also explains the small influence of the resonance decays on the *shape* of the rapidity distribution (Fig. 4), which is only scaled by the decay contributions.

In conclusion we have shown why the decay spectra are concentrated in the low- $m_T$  region. However, because of the superposition of many channels and the complex structure of the decay spectrum itself, we cannot estimate the influence by an easy method and have to resort to the full numerical evaluation of (4).

- [1] E. Schnedermann and U. Heinz, Phys. Rev. C **47**, 1738 (1993).
- [2] E. Schnedermann and U. Heinz, Phys. Rev. Lett. **69**, 2908 (1992).
- [3] E. Schnedermann and U. Heinz (unpublished).
- [4] A. Bamberger *et al.*, Phys. Lett. B **184**, 271 (1987); H. Ströbele *et al.*, NA35 Collaboration, Z. Phys. C **38**, 89 (1988); T. Åkesson *et al.*, NA34 Collaboration, *ibid.* **46**, 361 (1990); R. Albrecht *et al.*, WA80 Collaboration, *ibid.* **47**, 367 (1990).
- [5] J. Bächler *et al.*, NA35 Collaboration (submitted to Phys. Rev. Lett.).
- [6] J. Bartke *et al.*, NA35 Collaboration, Z. Phys. C **48**, 191 (1990).
- [7] H.v. Gersdorff *et al.*, Phys. Rev. C **39**, 1385 (1989).
- [8] K.S. Lee and U. Heinz, Z. Phys. C **43**, 425 (1989); K.S. Lee, U. Heinz, and E. Schnedermann, *ibid.* **48**, 525 (1990).
- [9] *Quark Matter '90*, Proceedings of the 8th International Conference on Ultrarelativistic Nucleus-Nucleus Collisions, Menton, France, 1990, edited by J.P. Blaizot *et al.* [Nucl. Phys. **A525** (1991)].
- [10] *Quark Matter '93*, Proceedings of the 10th International Conference on Ultrarelativistic Nucleus-Nucleus Collisions in Borlänge, Sweden, 1993 [Nucl. Phys. A (to be published)].
- [11] D. Röhrich, NA35 Collaboration, *Quark Matter '93* [10].
- [12] H. Ströbele, NA35 Collaboration, *Quark Matter '90* [9], p. 59c.
- [13] J.L. Goity and M. Leutwyler, Phys. Lett. B **228**, 517 (1989); M. Kataja and P.V. Ruuskanen, *ibid.* **243**, 181 (1990).
- [14] J. Schukraft, in *Quark Gluon Plasma Signatures*, edited by V. Bernard *et al.* (Editions Frontières, Strasbourg, 1990), p. 127; J. Simon-Gillo, *Quark Matter '93* [10].
- [15] G. Jancso *et al.*, Nucl. Phys. **B124**, 1 (1977); D. Drijard *et al.*, Z. Phys. C **9**, 293 (1981); M. Aguilar-Benitez *et al.*, *ibid.* **50**, 405 (1991); H. Grässler *et al.*, Nucl. Phys. **B132**, 1 (1978).
- [16] P. Koch, J. Rafelski, and W. Greiner, Phys. Lett. **123B**, 151 (1983).
- [17] J. Sollfrank, P. Koch, and U. Heinz, Phys. Lett. B **252**, 256 (1990); J. Sollfrank, P. Koch, and U. Heinz, Z. Phys. C **52**, 593 (1991).
- [18] H.W. Barz, G. Bertsch, D. Kusnezov, and H. Schulz, Phys. Lett. B **254**, 332 (1991); G.E. Brown, J. Stachel, and G.M. Welke, *ibid.* **253**, 315 (1991).
- [19] U. Ornik and R.M. Weiner, Phys. Lett. B **263**, 503 (1991).
- [20] J.D. Bjorken, Phys. Rev. D **27**, 140 (1983).
- [21] Yu.M. Sinyukov, V.A. Averchenkov, and B. Lörstadt, Z. Phys. C **49**, 417 (1991); M. Kataja, *ibid.* **38**, 419 (1988).
- [22] J. Letessier, A. Tounsi, U. Heinz, J. Sollfrank, and J. Rafelski, Phys. Rev. Lett. **70**, 3530 (1993); J. Letessier, A. Tounsi, U. Heinz, J. Sollfrank, and J. Rafelski, Paris Report No. PAR/LPTHE/92-27, 1992 (unpublished).
- [23] H.H. Gutbrod, A.M. Poskanzer, and H.G. Ritter, Rep. Prog. Phys. **52**, 1267 (1989); H.A. Gustaffson *et al.*, Phys. Rev. Lett. **52**, 1590 (1984); R.E. Renfordt *et al.*, *ibid.* **53**, 763 (1984).
- [24] H. Stöcker and W. Greiner, Phys. Rep. **137**, 277 (1986).
- [25] P.J. Siemens and J.O. Rasmussen, Phys. Rev. Lett. **42**, 880 (1979).
- [26] T. Abbott *et al.*, Phys. Rev. Lett. **64**, 847 (1990).
- [27] H. Stöcker, *Quark Matter '93* [10].
- [28] K. Werner, *Quark Matter '90* [9], p. 501c; K. Werner and P. Koch, Phys. Lett. B **242**, 251 (1990).
- [29] S. Wenig, Ph.D. thesis, Universität Frankfurt, 1990, GSI-Report GSI-90-23, 1990.
- [30] J.W. Cronin *et al.*, Phys. Rev. D **11**, 3105 (1975).
- [31] M.J. Longo, Nucl. Phys. **B134**, 70 (1978); A. Kryzwicki *et al.*, Phys. Lett. **85B**, 407 (1979).
- [32] C. De Marzo *et al.*, NA5 Collaboration, Phys. Rev. D **26**, 1019 (1982).
- [33] B. Alper *et al.*, Phys. Lett. **44B**, 521 (1973); M. Banner *et al.*, *ibid.* **44B**, 537 (1973).
- [34] P.V. Ruuskanen, Acta Physica Polonica **18**, 551 (1987).
- [35] F. Cooper and G. Frye, Phys. Rev. D **10**, 186 (1974).
- [36] Yu.M. Sinyukov, Z. Phys. C **43**, 401 (1989).
- [37] H.v. Gersdorff, in *Quark Matter '90* [9], p. 697c.
- [38] E. Schnedermann, Diploma thesis, Universität Regensburg, 1989.
- [39] E. Schnedermann, Ph.D. thesis, Universität Regensburg, 1992.
- [40] Particle Data Group, K. Hikasa *et al.*, Phys. Rev. D **45**, S1 (1992).